Vol. 402: 13–30, 2010
doi: 10.3354/meps08360

MARINE ECOLOGY PROGRESS SERIES
Mar Ecol Prog Ser

Published March 8

Primary production and plankton dynamics in the Reloncaví Fjord and the Interior Sea of Chiloé, Northern Patagonia, Chile

H. E. González[1,2,3,*], M. J. Calderón[1], L. Castro[2,4], A. Clement[5], L. A. Cuevas[6], G. Daneri[2,3], J. L. Iriarte[3,7], L. Lizárraga[2,3], R. Martínez[8], E. Menschel[1,2], N. Silva[9], C. Carrasco[9], C. Valenzuela[7], C. A. Vargas[3,8], C. Molinet[7]

[1]Instituto de Biología Marina, Universidad Austral de Chile, PO Box 567, Valdivia, Chile
[2]Centro COPAS de Oceanografía y COPAS Sur-Austral (PFB), Universidad de Concepción, PO Box 160-C, Concepción, Chile
[3]Centro de Investigación de Ecosistemas de la Patagonia (CIEP), Bilbao 449, Coyhaique, Chile
[4]Departamento de Oceanografía, Universidad de Concepción, PO Box 160-C, Concepción, Chile
[5]Plancton Andino, PO Box 823, Puerto Montt, Chile
[6]Department of Biology, University of Bergen, Jahnebakken 5, 5020 Bergen, Norway
[7]Instituto de Acuicultura, Universidad Austral de Chile, PO Box 1327, Puerto Montt, Chile
[8]Unidad de Sistemas Acuáticos, Centro de Ciencias Ambientales EULA, PO Box 160-C, Concepción, Chile
[9]Escuela de Ciencias del Mar, Pontificia Universidad Católica de Valparaíso, PO Box 1020, Valparaíso, Chile

ABSTRACT: Seasonal variability in freshwater discharge and solar radiation directly affects the structure and functioning of the pelagic community in Chile's northern Patagonian fjords. The input of fresh water loaded with silicate from the top and marine water enriched with nitrate and orthophosphate from the bottom results in overlapping limnetic and marine characteristics. Two research cruises (CIMAR 12) were conducted in the area of Reloncaví Fjord and the Interior Sea of Chiloé (42 to 44° S) during austral winter and spring 2006, in order to assess the spatial/temporal variability in biological, physical, and chemical oceanographic characteristics, and to quantify the carbon budget of the pelagic trophic webs in Reloncaví Fjord. Vertical flux of particulate organic carbon (POC) and primary production (PP) increased 2-fold (334 vs. 725 mgC m^{-2} d^{-1}) and 2 orders of magnitude (42 vs. 1893 mgC m^{-2} d^{-1}), respectively, from winter to spring. In addition, the bacterial secondary production to primary production (BSP:PP) ratio decreased from 3.7 to 0.2 in Reloncaví Fjord, suggesting a transition from microbial to classical pelagic food webs. The higher solar radiation and extended photoperiod of springtime promoted the growth of diatoms in a nutrient-replete water column. Allochthonous (river discharge) and autochthonous (phytoplankton exudates) organic matter maintained high year-round bacteria biomass and secondary production. In spring, grazing pressure from zooplankton on the microplankton (largely diatoms) resulted in the relative dominance of the classical food web, with increased export production of zooplankton faecal pellets and ungrazed diatoms. Conversely, in winter, zooplankton grazing, mainly on nanoplankton, resulted in a relative dominance of the microbial loop with lower export production than found in spring. Carbon fluxes and fjord-system functioning are highly variable on a seasonal basis, and both the multivorous trophic webs and the carbon export were more uncoupled from local PP than coastal areas.

KEY WORDS: Interior Sea of Chiloé · Patagonia marine ecosystem · Carbon budget

INTRODUCTION

Fjords and estuaries play an important role in biological productivity and carbon cycles in aquatic ecosystems worldwide. The productivity of Chilean fjords is influenced by oligotrophic freshwater discharge (rich in Si) from river runoff and glacial melting, as well as the vertical entrainment of Sub-Antarctic Water (SAAW) loaded with macronutrients from the adjacent oceanic area (Silva et al. 1997, 1998). The

*Email: hgonzale@uach.cl

magnitude of these inputs affects primary production (PP) through water column stratification and lateral advection, as determined by horizontal baroclinic changes. This physical scenario may have direct effects on the structure and functioning of the pelagic community, e.g. the succession of phytoplanktonic blooms during the productive season (spring) and the fate of the PP towards higher trophic levels versus its export to the sediments. The effect that the structure of micro- and mesozooplankton communities has on the routes by which the photosynthetically produced organic matter (OM) flows through the trophic web is well-known, as are the implications for retention versus export of organic particulate matter (Vargas & González 2004).

An integrated view of marine systems, with energy and matter inflow through classical and microbial food webs, has been used extensively to explain the fate of photosynthetically fixed OM in marine ecosystems (Calbet & Landry 2004). In highly productive coastal ecosystems, it has usually been assumed that PP supported mostly by diatoms might be efficiently transported to higher trophic levels through the so-called 'classical food web' (Ryther 1969) or exported from the productive layer as faecal material, detritus, or 'marine snow' (Turner 2002). In this context, the importance of bacteria and protozooplankton in the biogeochemical cycles of productive coastal marine systems has been widely accepted (Painting et al. 1992, Ducklow et al. 2001). The microbial loop may play a prominent role in productive systems, regulating the flow of OM in the water column and its transfer to higher trophic levels (Vargas et al. 2007, Paves & González 2008).

The Chilean fjord region (from 41 to 55° S) extends over >1600 km, contains 84 000 km of coastline, and covers 240 000 km^2 of highly complex geomorphological and hydrographic conditions. This region is characterised by strong climatic seasonal fluctuations (i.e. solar radiation and precipitation; Pickard 1971, Acha et al. 2004), partially modulating the seasonal changes in phytoplankton biomass and PP. Productivity estimations are relatively scarce for southern Chile (41 to 55° S) as compared with central-northern Chile (18 to 37° S). In the northern area of the Chilean fjords (41 to 48° S), PP and chlorophyll *a* (chl *a*) ranged from 1 to 26 mgC m^{-3} h^{-1} and from 1 to 12 mg chl *a* m^{-3} respectively (Pizarro et al. 2000, Iriarte et al. 2007). In addition, reports have shown that pico- and nanophytoplankton are dominant in the Strait of Magellan (53° S) after the spring bloom, whereas microphytoplankton contributes the bulk (>50%) of the pigment biomass in spring (Iriarte et al. 2001). Since spring blooms in middle and high latitude coastal regions play a pivotal role in carbon flows and ecosystem functioning (Tian et al. 2001), a better comprehension of the fate of PP is needed. Several studies report physical and chemical information for Reloncaví Fjord (Silva et al. 1997, Basten & Clement 1999, Silva & Palma 2006). However, thus far, no data have been reported on secondary bacterial production, planktonic trophic interactions, or the export of particulate organic matter (POM) in the framework of the microbial food web.

In the Patagonian fjords, the zooplankton community is usually dominated by dense aggregations of cladocerans and meroplanktonic crustacean larvae mixed with a diverse and abundant community of epipelagic calanoid copepods such as *Calanus australis*, *Calanoides patagoniensis* and *Drepanopus forcipatus* (Marín & Antezana 1985, Escribano et al. 2003, Rosenberg & Palma 2003). Zooplankton biomasses are higher in the Gulf of Ancud (mean 5.19 log DW 1000 m^{-3}) than in the Gulf of Corcovado (mean 4.92); the greater stability of the water column in the former microbasin seems to contribute to its high zooplankton biomass (Palma & Silva 2004). The abundant phytoplankton in spring and summer may, in turn, augment the abundance of planktonic herbivores and carnivores (Antezana 1999, Hamamé & Antezana 1999, Palma & Aravena 2001), crustacean larvae, and fishes (Balbontín & Bernal 1997, Mujica & Medina 2000). The latter are especially abundant in some channels that exchange an important amount of water with the adjacent oceanic area dominated by SAAW. Previous studies indicate that, in summer, the SAAW is highly productive, as evidenced by a high phytoplankton growth rate (Avaria et al. 1999, Pizarro et al. 2000). However, information on the fate of the photosynthetically generated carbon flows through the pelagic food web and their subsequent export to deeper layers of the fjords remains very scarce. This study aims (1) to assess the spatial and seasonal variability in the chemical, physical, and biological characteristics of Reloncaví Fjord and the Interior Sea of Chiloé and (2) to quantify the carbon budget of the pelagic trophic webs of Reloncaví Fjord in winter and spring. In particular, we set out to estimate the magnitude of the photosynthetic OM flowing through the classical and microbial food webs and the magnitude of the particulate organic carbon (POC) exported below the strong halocline.

MATERIALS AND METHODS

Two research cruises (CIMAR 12 Fiordos) were conducted in the area of Reloncaví Fjord (41° 38' S) and the Interior Sea of Chiloé (from 42 to 44° S) in austral winter (8–25 July 2006) and spring (4–12 November 2006) on board the AGOR 'Vidal Gormáz' of the Chilean Navy (Fig. 1). Three research approaches were implemented:

(1) Time-series stations. The Melinka meteorological station (43.8° S) was used to describe seasonal variability in solar radiation (2004 and 2005) (see Fig. 2a). The input of fresh water from the Puelo River was obtained from the Chilean General Water Directorate (DGA; www.dga.cl) for 2001 to 2007 (see Fig. 2b). A phytoplankton time-series station in Ilque Bay, Reloncaví Basin (41° 38′ S, 73° 05′ W), was used to describe the seasonal variability of diatoms (2001 to 2008) (see Fig. 2c). Weekly to monthly water samples were collected at the surface and at 5 and 10 m depth using a Go-Flo sampling bottle. From each depth, 200 ml were preserved in an acid Lugol's solution and later analysed for diatom counting using standard microscopy methods (Utermöhl 1958).

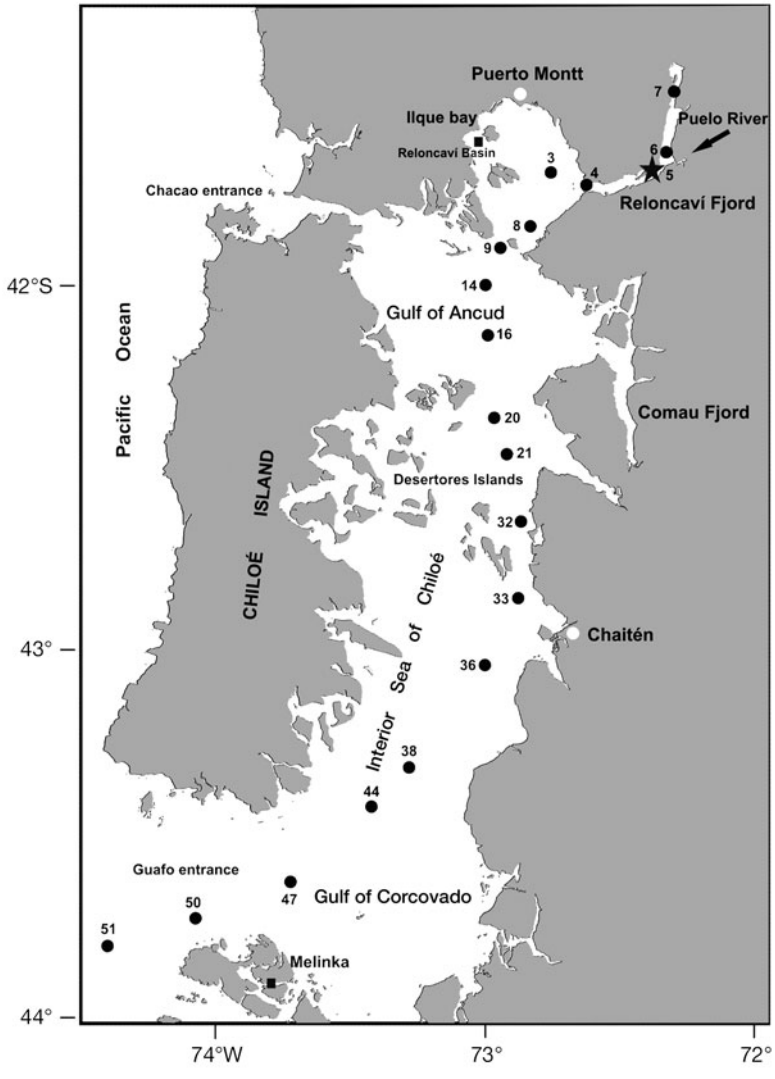

Fig. 1. Study area and stations (●) along the transect from the Reloncaví Fjord, through the Interior Sea of Chiloé to the Guafo entrance, Chile. Star: location of the process station (Stn 5); ■: locations of the diatom and solar radiation time-series stations in the Reloncaví Basin and at Melinka

(2) A transect of stations (from Reloncaví Fjord to the Guafo entrance). A long transect of stations was performed from the head of Reloncaví Fjord (Stn 7) to the coastal oceanic area at the Guafo entrance (Stn 50) (Fig. 1). At these stations, water samples for plankton (1, 5, 10, 25, 50 m) and dissolved inorganic nutrient analyses (1, 5, 10, 25, 50, 75, 100, 150, 200, 250, 300, 350 and 400 m) were collected at discrete depths (1, 5, 10, 25, 50 m) using a bottle-rosette system (details below). The physical structure of the water column (temperature, salinity, dissolved oxygen) was recorded with a Seabird 19 CTD. Salinity and oxygen sensors were calibrated by measuring salinity (with an Autosal salinometer) and dissolved oxygen (Winkler method) in discrete water samples.

(3) A process-oriented time-series station. This fixed station in the middle of Reloncaví Fjord (Stn 5) was used for a process-oriented study. The study was repeated 3 times (Days 1, 3 and 5) during a 5 d study program in winter and in spring. Stn 5, referred to as the 'process station', was used for the primary study of the possible fate of photosynthetically generated organic carbon through classical or microbial food webs. Here, we estimated the following processes: size-fractionated PP; bacterial secondary production (BSP); nano-, micro-, and mesozooplankton grazing; and vertical fluxes of particulates. In addition, we measured the following abundances and carbon-based biomasses: phytoplankton, bacteria, heterotrophic and autotrophic nanoflagellates (HNF, ANF), dinoflagellates and ciliates (see below).

The different physical, chemical and biological parameters measured/estimated during the winter and spring cruises are included in Table 1.

Size-fractionated chl *a* and POC. For chl *a* and phaeopigments, 200 ml seawater were filtered (MFS glass fibre filters, 0.7 µm nominal pore size) in triplicate and immediately frozen (–20°C) until later analysis by fluorometry, using acetone (90 % v/v) for the pigment extraction (Turner Design TD-700) according to standard procedures (Parsons et al. 1984). In addition, water samples were collected for POC concentrations in the water column. These samples (from 0.5 to 1.0 l) were filtered through precombusted MFS filters and stored frozen until later analysis following standard pro-

Table 1. Parameters measured/estimated during the winter (W) and spring (S) cruises at each station. Chl (fractionated chlorophyll *a*), POC (particulate organic carbon), Nut (nitrate, orthophosphate and silicic acid), BB (bacterial biomass), ANF-B (autotrophic nanoflagellate biomass), HNF-B (heterotrophic nanoflagellate biomass), Microzoo-B (microzooplankton biomass), Cop-B (copepod biomass), Eup-B (euphausiid biomass), HNF-G (heterotrophic nanoflagellate grazing), Microzoo-G (microzooplankton grazing, Cop-G (copepod grazing), Vert-F (vertical flux of particulates), PP (primary production) and BSP (bacterial secondary production)

Stn	Water column depth (m)	Lat. & long.	Chl	POC	Nut	BB	ANF-B	HNF-B	Micro-zoo-B	Cop-B	Eup-B	HNF-G	Micro-zoo-G	Cop-G	Vert-F	PP	BSP
3	238	41°40.52′S 72°45.54′W	W,S	W,S	W,S	W,S	W,S	W,S	W,S	W,S	W,S					W	W
4	455	41°42.92′S 72°38.53′W	W,S	W,S	W,S	W,S	W,S	W,S	W,S	S	S						
5[a]	255	41°41.21′S 72°24.87′W	W,S	W,S	W,S	W,S	W,S	W,S	W,S	W,S	W,S	W,S	W,S	W,S	W,S	W,S	W,S
6	196	41°35.42′S 72°20.39′W	W,S	W,S	W,S	W,S	W,S	W,S	W,S	S	S						
7	195	41°32.98′S 72°20.04′W	W,S	W,S	v	W,S	W,S	W,S	W,S	W,S	W,S						
8	112	41°45.23′S 72°50.95′W	W,S	W,S	W,S	W,S	W,S	W,S	W,S	S	S						
9	228	41°52.79′S 72°58.94′W	W,S	W,S	W,S	W,S	W,S	W,S	W,S	S	S						
14	362	41°58.75′S 72°59.55′W	W,S	W,S	W,S	W,S	W,S	W,S	W,S	S	W,S						
16	253	42°06.83′S 72°59.73′W	W,S	W,S	W,S	W,S	W,S	W,S	W,S	W,S	W,S						
20	240	42°20.15′S 72°55.88′W	W,S	W,S	W,S	W,S	W,S	W,S	W,S	S	S					W,S	W,S
21	126	42°34.82′S 72°54.39′W	W,S	W,S	W,S	W,S	W,S	W,S	W,S	W,S	W,S						
32	120	42°43.41′S 72°53.81′W	W,S	W,S	W,S	W,S	W,S	W,S	W,S	S	S						
33	142	42°53.35′S 72°53.33′W	W,S	W,S	W,S	W,S	W,S	W,S	W,S	W,S	W,S						
36	204	43°01.88′S 73°00.74′W	W,S	W,S	W,S	W,S	W,S	W,S	W,S	W,S	W,S						
38	179	43°13.94′S 73°17.05′W	W,S	W,S	W,S	W,S	W,S	W,S	W,S	W,S	W,S						
44	134	43°34.29′S 73°33.06′W	W,S	W,S	W,S	W,S	W,S	W,S	W,S	W,S	W,S					S	S
47	215	43°41.10′S 73°48.08′W	W,S	W,S	W,S	W,S	W,S	W,S	W,S	S	S						
49	225	43°41.31′S 74°07.35′W	S	S	S	S	S	S	S								
50	180	43°49.13′S 74°23.45′W	S	S	S	S	S	S	S								

[a]Process station

cedures (von Bodungen et al. 1991). For nutrient concentration analyses (nitrate, orthophosphate, silicic acid), water samples were collected using a CTD-rosette equipped with 24 Niskin bottles at the following depths: 1, 5, 10, 25, 50, 75, 100, 150, 200, 250, 300, 350 and 400 m, as far as possible depending on the water depth at each station. Water samples (50 ml) were stored at –20°C in acid-cleaned high-density polyethylene bottles and analysed in a nutrient autoanalyser (Mod. Technicon) according to Atlas et al. (1971).

Plankton abundance and biomass. Bacterioplankton, protozoan and phytoplankton counts were done with water samples collected at selected depths (0, 5, 10, 25, 50 m) in the upper 50 m of the water column. Bacterioplankton abundance (cells ml^{-1}) was measured on polycarbonate membrane filters (Nuclepore 0.2 µm) stained with the fluorochrome DAPI (Porter & Feig 1980) and using epifluorescence microscopy. Bacterial biomass was estimated using a factor of 20 fgC $cell^{-1}$ (Lee & Fuhrman 1987). For the enumeration of nanoflagellates, 20 ml sub-samples were filtered on a 0.8 µm polycarbonate membrane filter and stained with Proflavine (0.033% w/v in distilled water) according to Haas (1982) and fixed with glutaraldehyde. Sub-

samples for diatom counts (300 ml) were preserved in an acid Lugol's solution (1% final conc.). Sub-samples of 50 ml were placed in settling chambers for 30 h before analysis under an inverted microscope (Zeiss Axiovert 200, 400× magnification) using the standard methodology (Utermöhl 1958); a carbon:plasma volume ratio of 0.11 pgC μm^{-3} was applied for diatom carbon estimations (Edler 1979). For dinoflagellate and ciliate counts, 10 to 30 l of seawater from different depths (surface, 5, 10, 25 m) were filtered gently through a sieve (10 µm mesh size), then concentrated up to a final volume of ~100 ml and preserved with buffered formalin (5% final conc.). Carbon:plasma volume ratios of 0.3 and 0.19 pgC μm^{-3} were used for heavily thecate and athecate dinoflagellates forms, respectively (Lessard unpubl. data cited by Gifford & Caron 2000), and 0.148 pgC μm^{-3} was applied for ciliates (Ohman & Snyder 1991).

Zooplankton samples were collected by oblique tows using a Tucker trawl net (1 m^{-2} catching area, 300 µm mesh size) at night within the upper 75 m of the water column. Samples were preserved in borax buffered formalin (10% final conc.) for later analyses of the dominant zooplankton groups (large copepods and euphausiids). Additional tows using a WP-2 net (200 µm mesh size) were conducted to estimate the abundance of small calanoid copepods.

PP and BSP. Water samples for PP determinations were incubated in 100 ml borosilicate glass bottles (2 clear replicate bottles and 1 dark bottle for each depth) and placed in a natural-light incubator for 4 h (usually from 10:00 h to 14:00 h). The temperature was regulated by running surface seawater over the incubation bottles. For the subsurface chl *a* maximum, 40% and 2% light penetration incubation depths, light intensity was attenuated using a screen to approximate light at the depth where the water was collected. Sodium bicarbonate (40 µCi $NaH^{14}CO_3$) was added to each bottle. Following incubation, samples were manipulated under subdued light conditions prior to and after the incubation periods. The contents were filtered according to the fractionation procedures mentioned below. Filters (0.7 and 2.0 µm) were placed in 20 ml borosilicate scintillation vials and kept at –20°C until reading. To remove excess inorganic carbon, the filters were treated with HCl fumes for 4 h. A cocktail (10 ml, Ecolite) was added to the vials, and radioactivity was determined in a scintillation counter (Beckmann). Depth-integrated values of PP (mgC m^{-2} h^{-1}) were calculated using trapezoidal integration over the euphotic zone; the 4 depths considered were the surface, subsurface chl *a* maximum, and 40% and 2% surface irradiance depths. Integrated production rates per hour were multiplied by daily light hour for Reloncaví Fjord.

Phytoplankton size-fractionation was performed post-incubation in 3 sequential steps: (1) for the nanoplankton fraction (from 2.0 to 20 µm), seawater (125 ml) was pre-filtered using a 20 µm Nitex mesh and collected on a 2.0 µm Nuclepore; (2) for the picoplankton fraction (from 0.7 to 2.0 µm), seawater (125 ml) was pre-filtered using a 2.0 µm Nuclepore and collected on a 0.7 µm MFS glass fibre filter; and (3) for the whole phytoplankton community, seawater (125 ml) was filtered through a 0.7 µm MFS glass fibre filter. The microphytoplankton fraction was obtained by subtracting the production estimated in steps 1 and 2 from the production estimated in step 3.

BSP was estimated using water samples from the same oceanographic bottle as for PP experiments. The incorporation of L-[^{14}C(U)]-leucine into proteins (Simon & Azam 1989) was used to estimate BSP through the increment of biomass. Incubations were conducted at the *in situ* temperature and in darkness for 1 h, filtered over 0.22 µm membrane filters and extracted with cold 5% trichloroacetic acid (TCA). Samples were frozen on board and counted in a liquid scintillation counter in the laboratory. From each experiment, water samples were taken for bacteria cell numbers and biomass estimations.

The nanoflagellate and microzooplankton grazing experiments were performed using the size-fractionation method (Kivi & Setala 1995, Sato et al. 2007). Water samples were collected from the fluorescence maximum depth with a clean 10 l Go-Flo bottle-rosette system. After collection, seawater was size-fractioned by reverse filtration into 3 fractions: (1) <2 µm (i.e. mostly bacteria and cyanobacteria), (2) <10 µm (i.e. mostly bacteria, cyanobacteria, ANF, and HNF), and (3) <115 µm (i.e. the whole photoheterotrophic community). Grazing rates were calculated by comparing prey growth rates in the presence and absence of predators selected by reverse filtration as follows: for HNF grazing, by comparing (1) and (2); and for microzooplankton (ciliates + dinoflagellates) grazing on nanoflagellates (both ANF and HNF), by comparing (2) and (3) (Gifford 1993). Further descriptions of procedures and methods were fully described and published elsewhere (Vargas et al. 2008).

Copepod grazing. For copepod grazing estimations, animals were collected by slow vertical hauls in the upper 20 m of the water column using a WP-2 net (mesh size 200 µm) with a large non-filtering cod end (~40 l). Undamaged copepods were placed in 500 ml (from 4 to 8 small copepods) or 1000 ml (from 2 to 3 large copepods) acid-washed polycarbonate bottles. These bottles were filled with ambient water loaded with natural food assemblages of microplankton prescreened through a 200 µm net to remove most grazers. Three control bottles without animals and 3 bottles

with from 2 to 4 animals each were placed in an incubator rack on deck for approximately 19 to 25 h. The seawater incubation was mixed by hand every hour and, to some extent, by the ship's motion. Initial control bottles were immediately preserved with 2% acid Lugol's solution, and a sub-sample was also preserved in glutaraldehyde (as above). At the end of the incubation, sub-samples were taken from all the bottles and preserved in glutaraldehyde for nanoflagellate counts (20 ml) and acid Lugol's solution (60 ml, as above) for cell concentrations. Ingestion rates, measured as cell removal, were calculated according to Frost (1972), as modified by Marín et al. (1986).

Vertical flux of particulates. The vertical flux of POC was estimated by using surface-tethered, cylindrical sediment traps (122 cm^2 area and 8.3 aspect ratio) deployed at 50 m water depth at the 'process station' (Stn 5) for periods of 1 to 1.5 d. Sub-samples were used for microscopy using standard analysis (Utermöhl 1958); for POC, 0.5 to 1.0 l were filtered through precombusted MFS filters and stored frozen until later analysis.

RESULTS

Environmental conditions

The solar radiation recorded in the region (Melinka station) from 2004 to 2005 showed a highly seasonal variability, with lower values in winter (May–July: <400 µmol s^{-1} m^{-2}) and higher values in summer (December–February: 800 to 1000 µmol s^{-1} m^{-2}) (Fig. 2a). The average discharge from the Puelo River provided an input of 644 ± 155 m^3 s^{-1} fresh water (DGA, www.dga.cl, 2000 to 2007), reaching its highest points from June through July (winter) and from October through November (spring) and its lowest from February through April (from summer through autumn) (Fig. 2b). The annual cycle of total diatom abundance showed minimum and maximum values in austral winter (June–July: 0.5×10^9 to 1.4×10^9 cells m^{-2}) and spring (September–October: 13×10^9 to 18×10^9 cells m^{-2}); the 2 seasonal cruises (shaded areas in Fig. 2c) are typical of these periods.

At the transect, winter temperatures ranged from 8.7°C (Reloncaví Fjord) to 11.5°C (Guafo mouth). The thermocline from Reloncaví Fjord to the Desertores Islands was inverted, with lower temperatures (9 to 10°C) in the surface layer (<25 m) and higher temperatures at depth (>11°C). Below the surface layer, a vertical quasi-homogeneous thermal distribution (11°C) was found. In the Gulf of Corcovado, the whole water column was characterised by a quasi-homothermal vertical distribution (10.5°C) (Fig. 3A). In spring, the highest temperatures occurred at the surface in both Reloncaví Fjord and Basin (12.4°C), dropping to 11°C at 25 m depth and then remaining approximately constant down to the bottom. Similar temperatures characterised the whole water column from the Gulf of Ancud to the Gulf of Corcovado. Only the Guafo mouth showed lower temperatures (9.5°C) in the deeper waters (Fig. 4A).

In winter, the surface salinity ranged from 2.6 psu (Reloncaví Fjord) to 32.3 psu (Desertores Islands) (Fig. 3B). The vertical structure showed a strong halocline (from 3 to 32.5 psu) in the upper 25 m of Reloncaví Fjord and a relatively quasi homohaline (32.5 psu) from 25 m depth down to the bottom. The freshwater influence was noticed up to the Desertores Island, after which salinity fluctuated between 32 and 33 psu up to

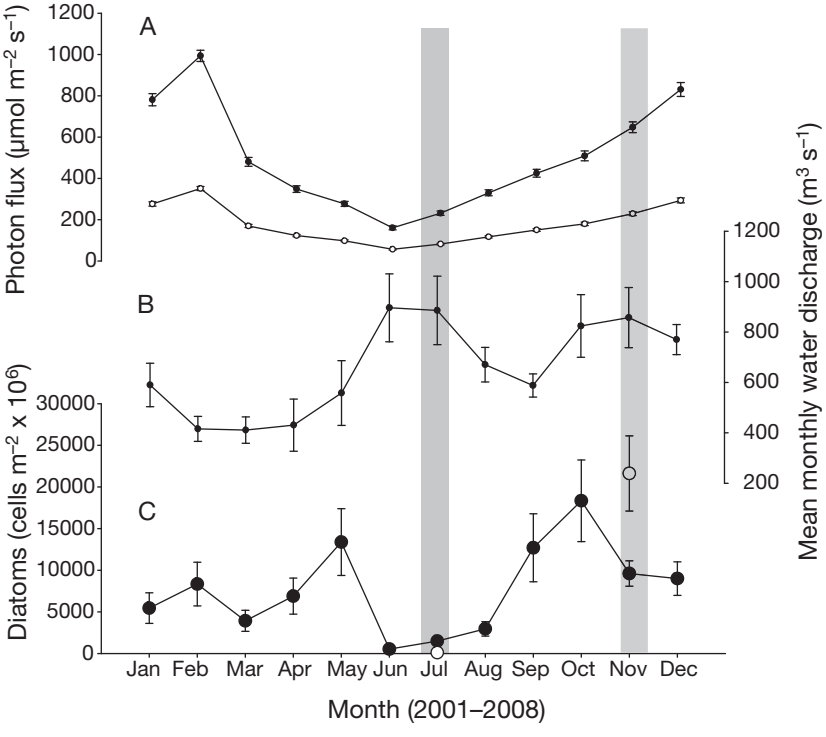

Fig. 2. (A) Average (2004–2005) monthly time series of solar radiation collected at the Melinka meteorological station (43.8° S) at the surface (●) and 10 m depth (○). (B) Average monthly Puelo River discharge determined near the river mouth (2000–2007) by the Chilean General Water Directorate (www.dga.cl). (C) Average monthly integrated diatom abundance (cells $m^{-2} \times 10^6$) in the upper 10 m of the water column around Stn 3 (2001–2008) (●). (○) Integrated diatom abundance at Stn 5 (process station) in July and November 2006. Vertical lines: standard error (n = 52); grey rectangular areas: periods in which the 2 CIMAR cruises were conducted in the study area

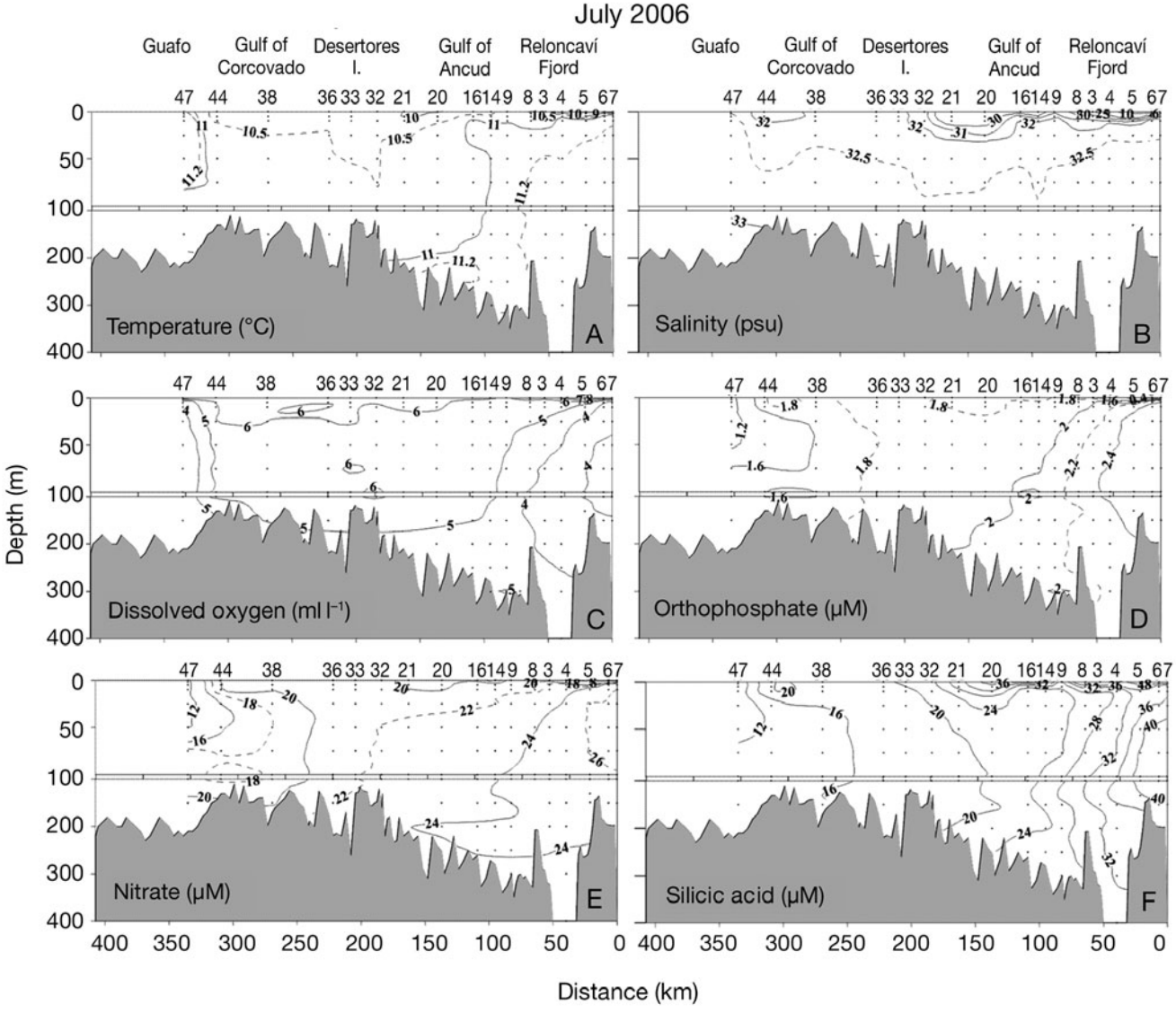

Fig. 3. Vertical distribution of the physical and chemical variables recorded along the transect depicted in Fig. 1 from Reloncaví Fjord (Stn 7) to the Guafo mouth (Stn 51) in the upper 400 m of the water column in July 2006. (A) Temperature, in °C, (B) salinity, in psu, (C) dissolved oxygen, in ml l^{-1}, (D) orthophosphate, in µM, (E) nitrate, in µM, and (F) silicic acid, in µM

the Guafo mouth (Fig. 3B). In spring, the situation was similar, although the vertical gradient in Reloncaví Fjord was slightly less pronounced than in winter (6 to 32.8 psu), and the salinity between Desertores Islands and the Guafo mouth fluctuated between 32 and 34 psu (Fig. 4B).

The highest wintertime surface dissolved oxygen concentrations were found in Reloncaví Fjord (8 ml l^{-1}) and the lowest (5.6 ml l^{-1}) in Ancud Gulf (Fig. 3C). In this area, an oxycline was observed between the surface and 25 m depth (8 and 4 ml l^{-1}, respectively). Similar concentrations (~6 ml l^{-1}) were found throughout the water column from Ancud Gulf to Corcovado Gulf (Fig. 3C). A less pronounced surface gradient was found in spring between Reloncaví Fjord (8.1 ml l^{-1}) and Ancud Gulf (6.3 ml l^{-1}). In addition, an oxycline from 8 to 4 ml l^{-1} was found within the upper 25 m of Reloncaví Fjord, remaining approximately constant below 25 m depth. From Ancud Gulf to Corcovado Gulf, the oxygen concentrations in the water column remained relatively constant at 6 ml l^{-1} (Fig. 4C).

The orthophosphate and nitrate concentrations in the surface waters ranged from 0.27 to 1.88 µM and from 2.6 to 21.6 µM in winter, respectively, and from 0.02 to 1.48 µM and from 0 to 12.6 µM in spring, respectively, with the lowest concentrations in Reloncaví Fjord and the highest around the Desertores Islands (Figs. 3D,E & 4D,E). On the other hand, the distributional pattern of silicic acid showed the highest concentrations in Reloncaví Fjord (up to 126 µM) and

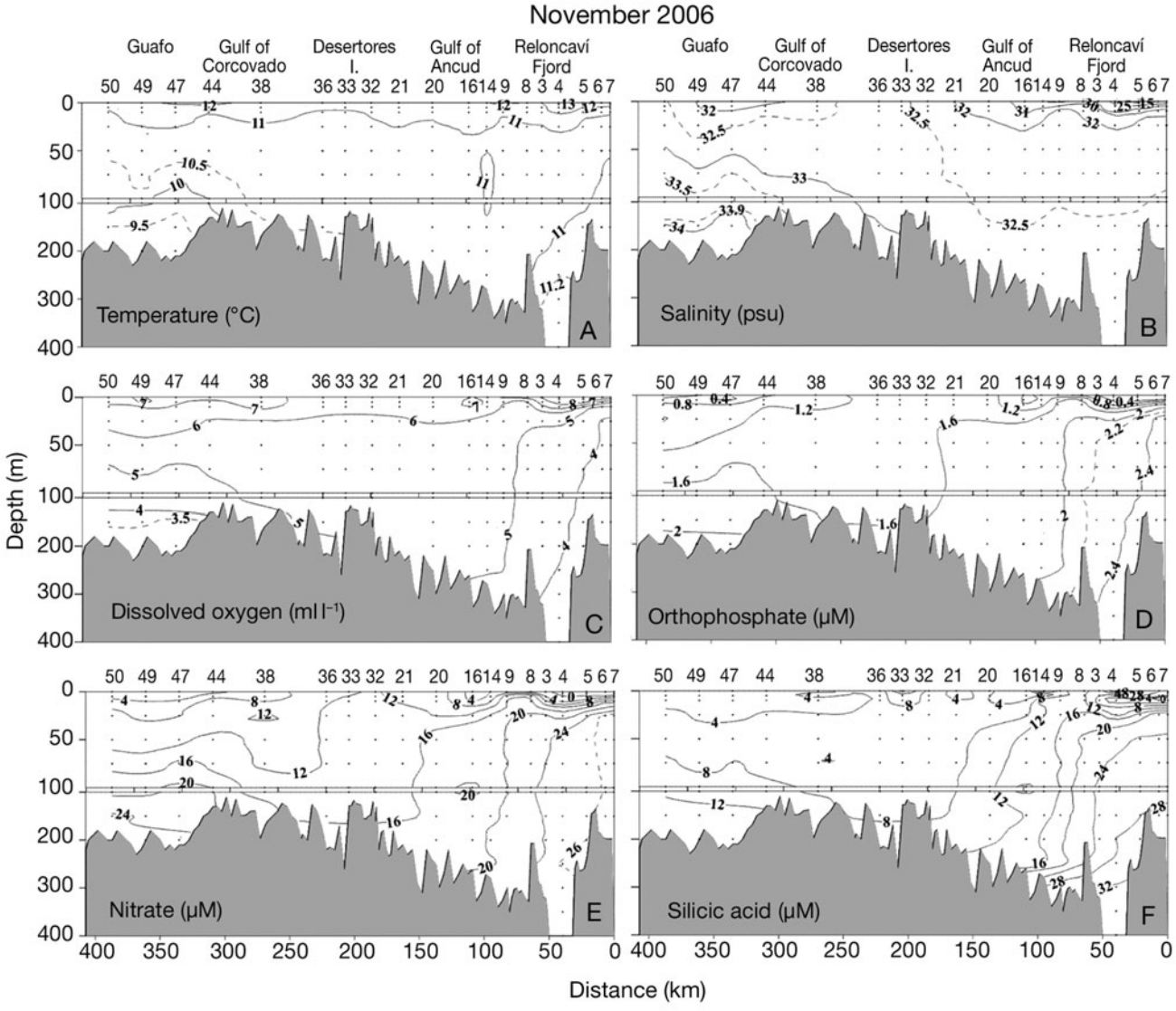

Fig. 4. Vertical distribution of the physical and chemical variables recorded along the transect depicted in Fig. 1 from Reloncaví Fjord (Stn 7) to the Guafo mouth (Stn 51)in the upper 400 m of the water column in November 2006. (A) Temperature, in °C, (B) salinity, in psu, (C) dissolved oxygen, in ml l^{-1}, (D) orthophosphate, in μM, (E) nitrate, in μM, and (F) silicic acid, in μM

the lowest in the Guafo mouth (9 μM) (Figs. 3F & 4F). The vertical distribution of inorganic nutrients in Reloncaví Fjord showed a 2-layer structure: the upper layer (<25 m depth) had low orthophosphate and nitrate (<2 and <22 μM, respectively) and high silicic acid (>40 μM) concentrations. The 2 former nutrients increased with depth (2.4 and 24 μM), whereas the latter decreased (<32 μM).

Chl *a* and POC concentrations

Conspicuous differences were found between winter and spring integrated (upper 25 m water column) chl *a* concentrations; the winter values (1 to 25 mg chl *a* m^{-2}) were 2 orders of magnitude lower than the spring ones (52 to 447 mg chl *a* m^{-2}). The vertical distribution of chl *a* showed a relatively homogeneous distribution within the upper 25 m in winter (0.02 to 0.2 mg chl *a* m^{-3}). A slight increase in concentration (0.2 to 2.0 mg chl *a* m^{-3}) was found in winter around Desertores Islands (Stn 5A) at 10 m depth. In spring, a conspicuous maximum was found in the chl *a* concentration at 10 m depth within Reloncaví Fjord (22 to 30 mg chl *a* m^{-3}). The chl *a* concentration decreased and became more shallow towards Reloncaví Basin and Desertores Islands (Fig. 6A), with values mainly between 5 and 10 mg chl *a* m^{-3} (at 0 to 15 m depth) and between 2 and

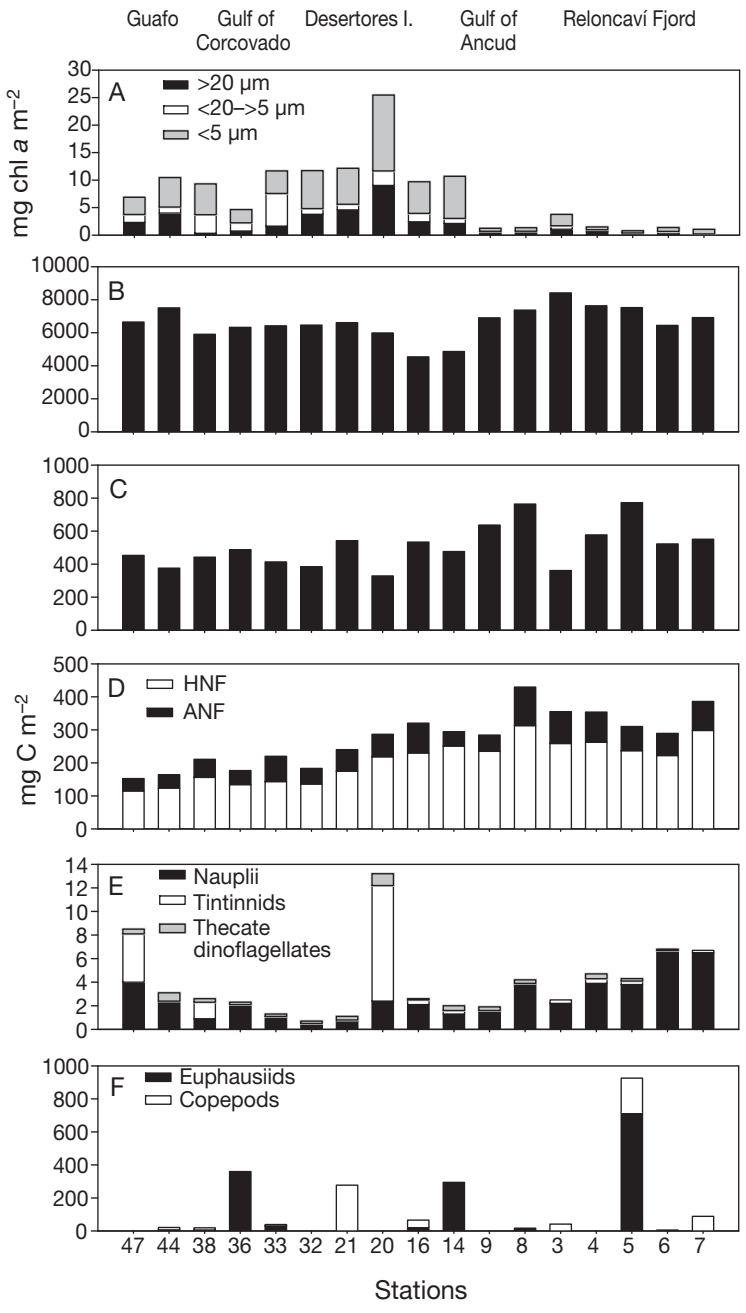

Fig. 5. Integrated values of different parameters measured during July 2006 along the transect from the Reloncaví Fjord to the Guafo entrance. (A) Size-fractionated chlorophyll *a*, (B) particulate organic carbon, (C) bacterial biomass, (D) heterotrophic and autotrophic nanoflagellates (HNF and ANF), (E) microzooplankton and (F) mesozooplankton. Abundances of the different groups of the plankton were transformed into carbon biomass by using the following equations: bacteria = 20 fgC cell^{-1} (Lee & Fuhrman 1987), flagellates = 6500 fgC cell^{-1} (Børsheim & Bratbak 1987), tintinnids = pgC = (µm^3) × 0.053 + 444.5 (Verity & Langdon 1984), thecate dinoflagellates = pgC = (µm^3) × 0.13 (Edler 1979), copepod nauplii = ngC = 1.51 × 10^{-5} LC$^{2.94}$ (LC: length of cephalothorax; Uye et al. 1996), calanoid copepods = 26.9 µgC cop^{-1} (González et al. 2000, Hirst et al. 2003), euphausiids = 3812 µgC euph^{-1} (N. Sánchez unpubl. data). All values were integrated into the upper 50 m of the water column, except chl *a*, integrated into the upper 25 m

5 mg chl *a* m^{-3} (at 15 to 25 m depth). The size-fractionated chl *a* was dominated by small phytoplankton (autotrophic flagellates <5 µm) in winter and large, chain-forming diatoms in spring. In winter, the contribution of the <5 µm, 5–20 µm and >20 µm size-fractions to the average total integrated chl *a* concentrations along the transect (7.3 mg chl *a* m^{-2}) were 54, 18 and 28%, respectively (Fig. 5A). In spring, the contribution of the same size-fractions to the average total integrated chl *a* concentrations along the transect (191.5 mg chl *a* m^{-2}) were 5, 4 and 91%, respectively (Fig. 6A).

In winter a few diatoms belonging largely to the genus *Skeletonema* and the species *Thalassionema nitzschioides* were present in the samples, while in spring, the microphytoplankton size-fraction (>20 µm) was dominated by chain-forming diatoms of the genera *Skeletonema*, *Chaetoceros*, *Thalassiosira* and *Rhizosolenia*. The highest diatom abundances were recorded in the surface waters within Reloncaví Fjord in spring (3 × 10^6 and 10 × 10^6 cells l^{-1}), whereas the lowest were recorded between the Desertores Islands and the Guafo mouth (0.1 × 10^6 to 1 × 10^6 cells l^{-1}). The winter abundances were 3 orders of magnitude less, ranging mainly from 1 × 10^3 to 4 × 10^3 cells l^{-1} throughout the study area.

Integrated POC concentrations in the upper 50 m of the water column were approximately one third in winter (4 to 8 gC m^{-2}) compared to spring (10 to 30 gC m^{-2}) (Figs. 5B & 6B). In winter, POC was highest in Reloncaví Fjord (mean ± SD: 7.3 ± 0.6 gC m^{-2}), decreased in the Gulf of Ancud (4.7 ± 0.2 gC m^{-2}), and increased again from the Desertores Islands to the Guafo entrance (6.5 ± 0.5 gC m^{-2}) (Fig. 5B). In spring, the concentrations in Reloncaví Fjord (25.0 ± 4.3 gC m^{-2}) were twice those of the Interior Sea of Chiloé from the Gulf of Ancud up to the Guafo entrance (Fig. 6B).

Plankton biomass (bacterioplankton, nanoflagellates, ciliates, mesozooplankton)

The integrated bacterioplankton biomass within the upper 50 m of the water column changed relatively little between the winter (range: 328 to 772 mgC m^{-2}; mean ± SD: 507 ± 129 mgC m^{-2}) and spring (303 to 925 mgC m^{-2}; mean ± SD: 431 ± 149 mgC m^{-2}) cruises (Figs. 5C & 6C). In addition, no clear spatial pattern could be identified, and bacterial biomass only repre-

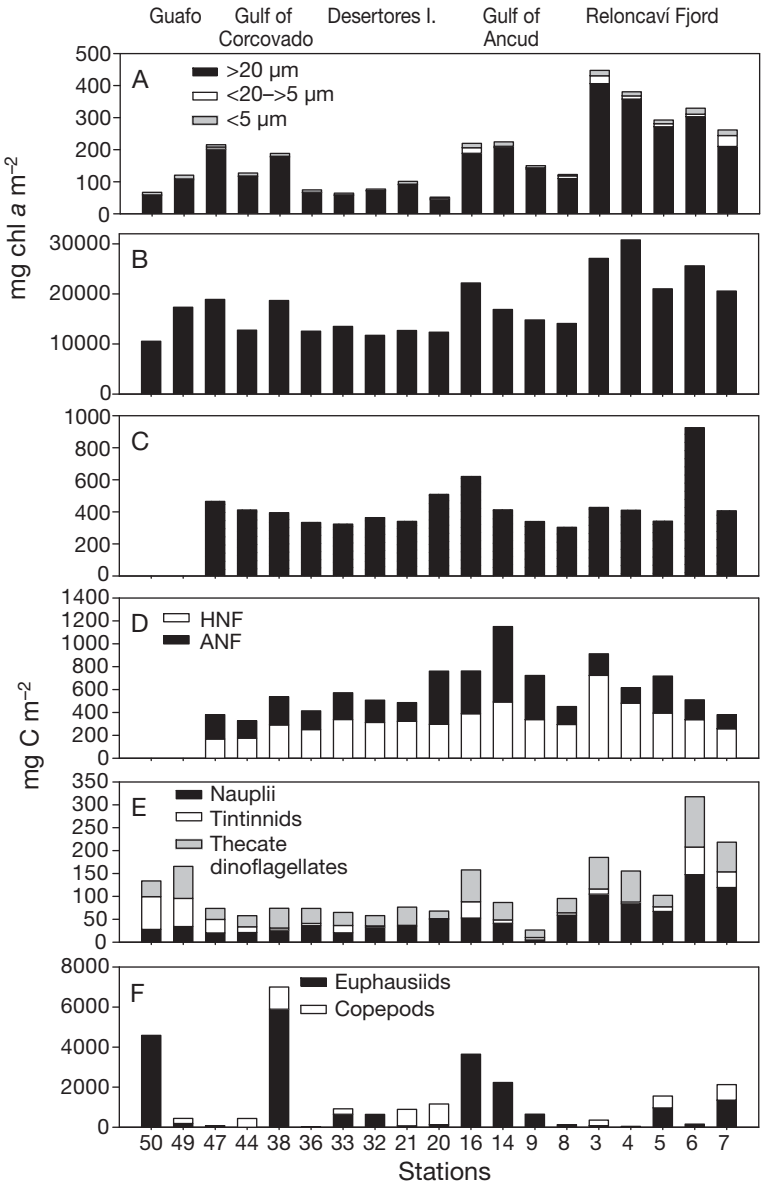

Fig. 6. Integrated values of different parameters measured during November 2006 along the transect from the Reloncaví Fjord up to the Guafo entrance. (A) Size-fractionated chlorophyll *a*, (B) particulate organic carbon, (C) bacterial biomass, (D) heterotrophic and autotrophic nanoflagellates (HNF and ANF), (E) microzooplankton and (F) mesozooplankton. Abundances of the different groups of the plankton were transformed into carbon biomass by using the equations given in Fig. 5

sents an average of 8% and 3% of POC during winter and spring, respectively. The integrated biomass of ANF increased 4-fold in spring (22 to 659 mgC m^{-2}; mean ± SD: 255 ± 143 mgC m^{-2}, Fig. 6D) as compared to winter (38 to 117 mgC m^{-2}; mean ± SD: 68 ± 23 mgC m^{-2}, Fig. 5D). The spatial distribution along the transect showed less biomass in the Gulf of Corcovado (Stns 38, 44 and 47) in winter (44 ± 9 mgC m^{-2}) and more biomass in the Gulf of Ancud (Stns 9, 14 and 16) in spring (472 ± 162 mgC m^{-2}, Figs. 5D & 6D). HNF were more evenly distributed in the study area, with winter values (115 to 299 mgC m^{-2}; 196 ± 55 mgC m^{-2}) approximately half those of springtime (168 to 626 mgC m^{-2}; mean ± SD: 331 ± 112 mgC m^{-2}). The overall integrated (upper 50 m water column) average microzooplankton abundance was higher in spring (21.0 ± 9.8 × 10^6 ind. m^{-2}) than in winter (1.2 ± 1.4 × 10^6 ind. m^{-2}). The dominant taxa in spring were the thecate dinoflagellate genera *Diplopsalis* and *Protoperidinium*, whereas, in winter, tintinnids (genus *Salpingella*) and thecate dinoflagellates (genera *Ceratium* and *Protoperidinium*) dominated at Stns 44 and 20. In terms of biomass, the copepod larval stages (nauplii) dominated in both winter (2.7 mgC m^{-2}) and spring (53.1 mgC m^{-2}, Figs. 5E & 6E). The integrated copepod abundance within the upper 50 m of the water column showed no evidence of vertical migration and, numerically, *Paracalanus parvus*, copepodites and *Calanus* spp. were predominant. In winter, these taxa showed average abundances (day and night catches) of 2163, 2535 and 2959 ind. m^{-2}, respectively, and, in spring, of 8255, 5133 and 1995 ind. m^{-2}. The species that showed the highest seasonal variability was *Rhyncalanus gigas*, increasing from an average abundance of 54 ind. m^{-2} in winter to 1571 ind. m^{-2} in spring. The average integrated copepod biomass in the study area increased 7-fold from winter (86 mgC m^{-2}) to spring (617 mgC m^{-2}). The integrated euphausiid abundance within the upper 50 m of the water column at Stn 5 was significantly higher in spring (626 ind. m^{-2}) than in winter (321 ind. m^{-2}), largely represented by *Euphausia vallentini* (>90%). For the whole study area, the average carbon biomass was 105 and 940 mgC m^{-2}, for winter and spring, respectively (Figs. 5F & 6F).

Productivity, pelagic food web and carbon export flux

The PP at Stn 5 increased by up to 2 orders of magnitude from winter to spring, with mean ± SD of 42.4 ± 5.7 mgC m^{-2} d^{-1} and 1893.0 ± 1549.0 mgC m^{-2} d^{-1} respectively (Table 2). In winter, the PP increased slightly near the Gulf of Ancud and the Desertores Islands

(115.1 mgC m^{-2} d^{-1} and 185.4 mgC m^{-2} d^{-1} at Stns 3 and 20 respectively), whereas, in spring, higher PP values were located close to the Desertores Islands and the Gulf of Corcovado (2476.0 mgC m^{-2} d^{-1} and 5476.6 mgC m^{-2} d^{-1} at Stns 20 and 44 respectively). On average, the size-fractions that contributed to the bulk of PP were nanophytoplankton (in winter, 78.3% of the total PP) and microphytoplankton (in spring, 84.5%, Table 2).

In winter and spring 2006, the BSP at Stn 5 averaged 157.2 ± 28.1 and 437.2 ± 138.9 mgC m^{-2} d^{-1}, respectively (n = 3, Table 2). In winter, similar values were found in Reloncaví Basin (278.7 mgC m^{-2} d^{-1}), contrasting with the very low values found around the Desertores Islands (20.5 mgC m^{-2} d^{-1}). The relatively high values of BSP in spring seemed to be restricted to the area inside Reloncaví Fjord (Stn 5), with low BSP values characterising the Desertores Islands (Stn 20, 42.6 mgC m^{-2} d^{-1}) and the Guafo entrance (Stn 44, 26.1 mgC m^{-2} d^{-1}, Table 2).

HNF was very abundant year-round, but bacterivory rates were higher in winter than in spring (12 to 19 vs. 0.01 to 0.3 bacteria ind.$^{-1}$ h^{-1} or 7.5×10^{-9} vs. 7.2×10^{-11} mgC ind.$^{-1}$ d^{-1}, Table 3A), resulting in higher integrated grazing rates for winter (>100% of the BSP) than spring (<1% of the BSP, Fig. 7). The microzooplankton (<115 µm) consisted mainly of choreotrich ciliates such as *Strombidium* spp. and naked dinoflagellates such as *Gymnodinium* spp. in winter, and thecate dinoflagellates such as *Protoperidinium* spp. and *Prorocentrum micans* in spring. In this productive period, thecate dinoflagellates and tintinnids reached abundances up to 1.2×10^7 ind. m^{-2} in the upper 50 m water column of the process station (Stn 5), 2 orders of magnitude lower than the small (<20 µm) naked dinoflagellates (data not shown). At Stn 5, the microzooplankton removed HNF at a rate of 8×10^{-6} mgC ind.$^{-1}$ d^{-1} in spring and 1.8×10^{-5} mgC ind.$^{-1}$ d^{-1} in winter (Table 3A). Low average copepod ingestion rates were estimated in winter (6×10^{-5} mgC ind.$^{-1}$

Table 2. Average and standard deviation of total and fractionated primary production (PP) and bacterial secondary production (BSP) during the winter and spring cruises. Values are given in mgC m^{-2} d^{-1}. nd = no data. Values between brackets denote % of total PP

	Stn 5	Stn 3	Stn 20	Stn 44
Winter				
PP				
>23 µm	2.0 ± 2.9 (4.7)	7.4 (6.4)	45.3 (24.4)	nd
5–23 µm	33.2 ± 10.4 (78.3)	86.8 (75.1)	100.4 (54.2)	nd
<5 µm	7.2 ± 4.1 (17.0)	21.3 (18.4)	39.7 (21.4)	nd
Total	42.4	115.1	185.4	nd
BSP	157.2	278.7	20.5	nd
Spring				
PP				
>23 µm	1599.0 ± 1654.8 (84.5)	nd	1599.0 (75.1)	4662.7 (85.1)
5–23 µm	171.3 ± 63.4 (9.0)	nd	570.3 (23.0)	603.5 (11.0)
<5 µm	122.8 ± 44.6 (6.5)	nd	46.8 (1.9)	210.4 (3.9)
Total	1893	nd	2476	5476.6
BSP	437.2	nd	42.6	26.1

Table 3. Average individual grazing rates (mgC ind.$^{-1}$ d^{-1}), average integrated (upper 50 m water column) abundance (ind. m^{-2}), and average grazing rates exerted by the integrated communities (mgC m^{-2} d^{-1}) of heterotrophic nanoflagellates (HNF), microzooplankton (Microzoo), copepods and euphausiids during the winter and spring cruises at the 'process station' (Stn 5). The vertical flux of particulates was 334.1 ± 69.2 mgC m^{-2} d^{-1} (n = 6) in winter and 725.3 ± 220.7 mgC m^{-2} d^{-1} (n = 12) in spring

Plankton taxon	Cruise season	Grazing rate: Individual (mgC ind.$^{-1}$ d^{-1})	Grazing rate: Community (mgC m^{-2} d^{-1})	Abundance (ind. m^{-2})
HNF	Winter	7.5×10^{-9} [a]	226.5	3.02×10^{10}
	Spring	7.2×10^{-11} [b]	3.7	5.09×10^{10}
Microzoo	Winter	1.8×10^{-5} [c]	1.7[i]	9.3×10^{4} [i]
			11.78[j]	1.57×10^{9} [c]
	Spring	8×10^{-6} [d]	96.0[i]	1.2×10^{7} [i]
			0.2[j]	2.13×10^{9} [k]
Copepods	Winter	6×10^{-5} [e]	0.03	472[l]
	Spring	6×10^{-3} [f]	19	3143[l]
Euphausiids	Winter	0.05[g]	16	321
	Spring	0.07[h]	44	626

[a]Range: 12 to 19 bacteria HNF^{-1} h^{-1} (or 6×10^{-9} to 9×10^{-9} mgC ind.$^{-1}$ d^{-1})
[b]0.01 to 0.3 bacteria HNF^{-1} h^{-1} (or 4.8×10^{-12} to 144×10^{-12} mgC ind.$^{-1}$$d^{-1}$)
[c]0.5 to 1.0 ngC ind.$^{-1}$ h^{-1}
[d]6.5 to 9.6 ngC ind.$^{-1}$ d^{-1}
[e]0.02 to 0.1 µgC ind.$^{-1}$ d^{-1}
[f]2 to 10 µgC ind.$^{-1}$ d^{-1}
[g]Average of *E. vallentini* juveniles and adults: 0.0518 mgC ind.$^{-1}$ d^{-1} (Sánchez 2007)
[h]Average *Euphausia vallentini* juveniles and adults: 0.0667 mgC ind.$^{-1}$ d^{-1} (Sánchez 2007)
[i]Tintinnids and thecate dinoflagellates >20 µm
[j]Naked dinoflagellates <20 µm (assuming an ingestion rate similar to HNF)
[k]Naked dinoflagellates <20 µm
[l]*Paracalanus parvus* and *Calanus* spp.

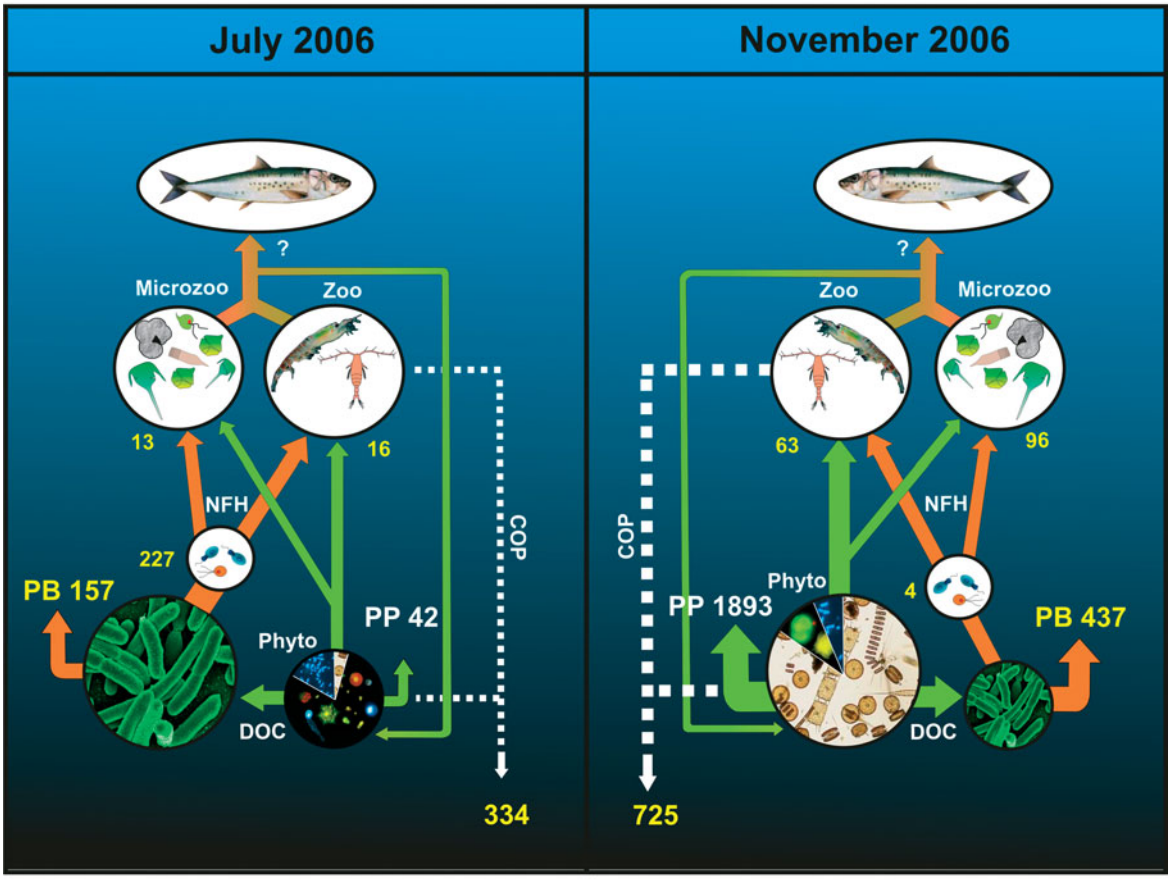

Fig. 7. Conceptual model of carbon flow in Reloncaví Fjord, showing the average values of primary production (PP), bacterial secondary production (BSP), vertical carbon flux, and grazing rates through heterotrophic nanoflagellates (HNF), microzooplankton (Microzoo), and copepods/euphausiids (Zoo) during the study programs conducted at Stn 5 in July and November 2006. All values are given in mgC m^{-2} d^{-1}. PB, DOC, Phyto, COP and NFH refer to bacterial secondary production, dissolved organic carbon, phytoplankton, particulate organic carbon and heterotrophic nanoflagellates, respectively

d^{-1}), whereas, in spring, small copepods such as *Paracalanus parvus* and large copepods such as *Calanus chilensis* and *Rhyncalanus nasutus* ingested an average of 6×10^{-3} mgC $ind.^{-1}$ d^{-1} (Table 3A). The average ingestion rates reported for *Euphausia vallentini* juveniles and adults (Sánchez 2007) in Comau Fjord, located beside Reloncaví Fjord (see Fig. 1), were integrated for the upper 50 m of the water column using only the euphausiid abundances recorded in the samples collected during night catches (due to their pronounced vertical migration). Thus, the integrated euphausiid ingestion rates were considerably lower in winter (16 mgC m^{-2} d^{-1}) than in spring (44 mgC m^{-2} d^{-1}, Table 3C). The vertical flux of particulates in July (334.1 ± 69.2 mgC m^{-2} d^{-1}, n = 6) was half that in November 2006 (725.3 ± 220.7 mgC m^{-2} d^{-1}, n = 12), with faecal pellets from zooplankton making the dominant contribution to the vertical carbon flux (Table 3C).

DISCUSSION

The rugged coastline of the study area is characterised by (1) a physical scenario impinged on by the freshwater inflow of the Puelo River (644 m^3 s^{-1}, Fig. 2b) and (2) a geomorphological scenario consisting of 4 different areas with different connections between them: (A) Reloncaví Fjord, with an E-W orientation, (B) the semi-enclosed Reloncaví Basin and Interior Sea of Chiloé, including 2 microbasins: (C) the Gulf of Ancud in the north and (D) the Gulf of Corcovado in the south; the latter 2 are separated by the Desertores Islands. The SAAW that penetrates the study area from the north (Chacao entrance) and the south (Guafo entrance) mixes with fresh waters coming from rivers, generating a lower salinity water mass (31 to 33 psu) known as Modified Sub-Antarctic Water (MSAAW); the MSAAW fills the microbasins from the Gulf of Corcovado to Reloncaví Fjord (Silva et al. 1998). In addi-

tion, the area from Reloncaví Fjord to the Gulf of Corcovado is influenced by a strong freshwater gradient and the stratification of the upper water column; i.e. the vertical extension of the upper brackish layer is reduced due to a spring–summer shortage in the freshwater inflow (reduced precipitation) that increases salinity from 10 psu (in winter) to 15 psu. Overall, a freshwater layer loaded with silicic acid is found within the upper 4 to 7 m of the water column. This layer is separated from a marine water layer loaded with nitrate and orthophosphate by a strong pycnocline, resulting in overlapping limnetic and marine characteristics in the Fjord and Interior Sea of Chiloé (Silva & Neshyba 1979, Silva et al. 1998).

In the scenario described above, PP is high (>1 gC m^{-2} d^{-1}) in spring, summer and early autumn (our Table 2; Iriarte et al. 2007), decreasing sharply in late autumn and winter. As the macronutrient concentration in the study area does not seem to be limiting, the changes observed in PP seem to be tied more to seasonal changes in the light regime than to the nutrient availability (see below). In line with this, the relatively low average values of the C:chl *a* ratio in the upper 10 m of the water column along the transect in spring (87) contrast with the high average value in winter (487). In general, low values have been reported for other estuarine systems during the productive season (Table 4), and high values in winter, when allochthonous OM input (probably loaded with refractory carbon) increased during the period of high river discharges.

Along with an increase of up to 2 orders of magnitude in total chl *a* concentrations from winter to spring, the size-fraction distribution shifted conspicuously with the dominance of nano- and microphytoplankton, respectively. Up to 2 orders of magnitude in pigment concentrations have been reported within a time scale of a few days during the onset and decay of a *Skeletonema costatum* bloom in the Ría de Vigo, Spain (Álvarez-Salgado et al. 2005 and our Table 4). In our study area, the high pigment biomass in spring was due to the proliferation of chain-forming diatoms, notably from the genera *Thalassiosira*, *Chaetoceros* and *Skeletonema*. The same diatom genera have been described as very abundant in coastal areas off central Chile (González et al. 1987, 1989) and in several disparate fjords such as those located in Newfoundland, Canada (Thompson et al. 2008). The continuous supply of fresh water loaded with silicic acid (Figs. 3 & 4) and the increased solar radiation (Fig. 2A) and photoperiod seem to favour the development of large, filamentous diatom blooms during the productive period. Although cells of diatom species such as *Skeletonema costatum* (dominant in the area) are able to germinate under low light (i.e. 65 µm quanta m^{-2} s^{-1}), a higher light threshold is needed for rapid growth (>280 µm quanta m^{-2} s^{-1}) (Shikata et al. 2008). This threshold was surpassed only in spring and summer in the study area (Fig. 2A). Here, silicic acid (4 to 126 µM l^{-1}), nitrate (0.5 to 26 µM l^{-1}) and orthophosphate (0.4 to 2.4 µM l^{-1}) concentrations were always higher than their respective half-saturation uptake concentrations by *S. costatum* (0.8 µM l^{-1}, Paasche 1973; 0.4 µM l^{-1}, Eppley et al. 1969; 0.68 µM l^{-1}, Tarutani & Yamamoto 1994) (Figs. 3 & 4). The only possible orthophosphate limitation might have occurred within the upper 5 m of the water column (well within the freshwater layer) inside Reloncaví Fjord (Stns 4 to 7), but, overall, all the macronutrients appear to be non-limiting factors, as their levels are sufficient for growth.

The winter and spring average bacterioplankton biomasses (507 and 431 mgC m^{-2}, respectively; Figs. 5C & 6C) and secondary productivity (157.2 and 437.2 mgC m^{-2} d^{-1}, respectively; Table 2, Fig. 7) did not differ substantially and were well within the values reported for Chile's central-northern upwelling areas (262 to 1274 mgC m^{-2}, Troncoso et al. 2003). It seems that the higher grazing pressure done by HNF over heterotrophic bacteria during winter (Table 3A,C) has a key role controlling BSP and growth during this season. The reduced HNF grazing pressure and the higher availability of inorganic nutrients and C sources allowed a higher BSP during springtime.

The relative constancy shown by bacterial activity contrasts markedly with the seasonal changes in PP, which differs by 1 or 2 orders of magnitude from the non-productive (winter) to the productive (spring) season. Whereas the PP observed in spring can easily account for the BSP, in winter, a subsidy of dissolved organic matter (DOM) from Patagonian rivers (Perakis & Hedin 2002, Pantoja et al. in press) needs to be invoked. The freshwater input might constitute an important flux of DOM/POM and macro- and oligoelements to coastal areas (Raymond & Bauer 2000); these factors are still absent from or scarcely represented in global biogeochemical models. For instance, if we use a conservative estimate for dissolved organic carbon (DOC) of 8.200 mgC m^{-3} (Pantoja et al. in press), the Puelo River would discharge 456 tC d^{-1}. POC concentrations were always high, and an important fraction was probably introduced into the fresh water loaded with OM (allochthonous OM). In addition, in estuarine systems, microbes as well as mesozooplankton might rely on this OM for from 5 to 80% of their production, which increases exponentially with increasing river discharge (Maranger et al. 2005, Hoffman et al. 2008). Overall predominant is the idea that in estuarine systems, allochthonous inputs of OM are more important quantitatively, but autochthonous OM likely provides more readily available substrates for

Table 4. Comparison of the parameters estimated in this study with those of other fjord and estuarine systems: fractionated chlorophyll *a* concentration (Chl *a*), particulate organic carbon concentration (POC-C), nutrient concentration (Nutrient-C), carbon-to-chlorophyll ratio (C:chl *a*), bacterial biomass (BB), microzooplankton biomass (Microzoo-B), copepod biomass (Copepod-B), copepod grazing rate (Copepod-G), vertical flux of particulates (Vertical-F), primary production (PP), bacterial secondary production (BSP)

Parameter (units)	Season, month, place, country	Source	Present study (total average, winter–spring)
Chl *a* (mg m^{-2})			
104	August–September, Skagerrak	Maar et al. (2004)	7–192 mg m^{-2}
21–25	July, Sandsfjord, Norway	Nielsen & Andersen (2002)[a]	
127	April, Balsfjord, Ullsfjord & Malangen, Norway	Archer et al. (2000)	
8–279	February, Ría de Vigo, Spain	Álvarez-Salgado et al. (2005)	
POC-C (mgC m^{-2})			
6224–24 942	April, Balsfjord, Ullsfjord & Malangen, Norway	Archer et al. (2000)[b]	6619–17 969 mgC m^{-2}
Nutrient-C (µM)			
NO^3 + NO_2 (0.32); $Si(OH)_3$ (0.77)	August–September, Skagerrak	Maar et al. (2004)	See Figs. 3 & 4
C:chl ratio			
108	August–September, Skagerrak	Maar et al. (2004)	487–87 mgC m^{-2}
BB (mgC m^{-2})			
833	August–September, Skagerrak	Maar et al. (2004)	507–431 mgC m^{-2}
178	April, Balsfjord, Ullsfjord & Malangen, Norway	Archer et al. (2000)[c]	
145	July, Aysén Fjord, Chile	H. González (unpubl. data)	
222	November, Aysén Fjord, Chile	H. González (unpubl. data)	
Microzoo-B (mgC m^{-2})			
121–268	July, Sandsfjord, Norway	Nielsen & Andersen (2002)	278–696 mgC m^{-2}
1507	April, Balsfjord, Ullsfjord & Malangen, Norway	Archer et al. (2000)[c]	
Copepod-B (mgC m^{-2})			
1216–1798	August–September, Skagerrak	Maar et al. (2004)	86–617 mgC m^{-2}
453–1882	July, Sandsfjord, Norway	Nielsen & Andersen (2002)	
Copepod-G (mgC m^{-2} d^{-1})			
400–1211 (20–92% of PP)	August–September, Skagerrak	Maar et al. (2004)	0.03–19 mgC m^{-2} d^{-1} (*Acartia* and *Calanus* spp.)
<2% PP	February–March, Kattegat	Nielsen & Richardson (1989)	
Vertical-F (mgC m^{-2} d^{-1})			
168–708 (32–59% of PP)	August–September, Skagerrak	Maar et al. (2004)	334–725 mgC m^{-2} d^{-1}
58	April, Bjørnajforden, Norway	González et al. (1994)	
99	April–May, Baltic Sea	Smetacek et al. (1978)	
196	November, Comau Fjord, Chile	González et al. (2009)	
PP (mgC m^{-2} d^{-1})			
1096	August–September, Skagerrak	Maar et al. (2004)	114–3282 mgC m^{-2} d^{-1}
2788	April, Balsfjord, Ullsfjord & Malangen, Norway	Archer et al. (2000)	
300–7260	February, Ría de Vigo, Spain	Álvarez-Salgado et al. (2005)	
220	November, Comau Fjord, Chile	J. Iriarte (unpubl. data)	
200	July, Puyuhuapi Fjord, Chile	G. Daneri (unpubl. data)	
1200	November, Puyuhuapi Fjord, Chile	G. Daneri (unpubl. data)	
BSP (mgC m^{-2} d^{-1})			
244	August–September, Skagerrak	Maar et al. (2004)	152–169 mgC m^{-2} d^{-1}
477–871	April–October, Hudson River, USA	Maranger et al. (2005)	
20	July, Puyuhuapi Fjord, Chile	G. Daneri unpubl. (data)	
750	November, Puyuhuapi Fjord, Chile	G. Daneri unpubl. (data)	

[a]Assuming C:chl ratio of 104
[b]Integrated in the upper 20 and 170 m
[c]Integrated in the upper 20 m

bacteria (Maranger et al. 2005). In the study area, the analysis of surface sediment cores showed a land-ocean gradient in the $\delta^{13}C$ values from –24.2‰ within the Reloncaví Fjord, –22.4‰ in the Reloncaví Basin, –21.1‰ in the Corcovado Gulf, and –19.6‰ in the Guafo entrance (Silva et al. 2009). In the vicinity of Stn 6, this value increased with core-depth, from –23‰ in the surface up to –26‰ at 40 cm depth (~400 yr ago), denoting a reduction in the allochthonous influence during the last 4 centuries (L. Rebolledo unpubl. data), a situation that has been paralleled by streamflow reductions in the Puelo River discharges since 1600 (Lara et al. 2008).

In the Baker River estuary, located south of the study area (47°47´S), between 20 and 50% of the total copepod ingestion, in terms of daily body carbon, has been estimated to be associated with allochthonous terrigenous sources. This finding was based on an isotopic analysis of small (*Acartia tonsa* and *Paracalanus parvus*) and large (*Calanus* spp.) copepods, which showed $\delta^{13}C$ ranging from –21 to –24‰ within time scales of a few days. These results also showed that during relatively short periods of time, copepods may switch from low microplankton (diatoms and flagellates of marine origins) ingestion (~1 to 2 µgC ind.$^{-1}$ d^{-1}) and slightly depleted $\delta^{13}C$ values (–24‰), to high microplankton ingestion (~4 and 12 µgC ind.$^{-1}$ d^{-1}) and enriched $\delta^{13}C$ values (–21‰) (C. Vargas unpubl. data). This might imply that copepod dependence on allochthonous sources of organic carbon declines with increasing fjord trophy (or microplankton availability). In addition, these results suggest that a significant proportion of the OM in Chilean fjords had an allochthonous origin and can be channelled either directly to higher trophic levels (zooplankton and fishes) through the ingestion of detrital particles, or through the microbial food webs (i.e. allochthonous DOC — bacteria — HNF — Zooplankton).

During this study, large thecate dinoflagellates (mainly of the genera *Protoperidinium* and *Ceratium*) were relatively scarce (<0.1 cell l^{-1}) compared to the small (<20 µm) naked dinoflagellates (~3 × 10^4 cells l^{-1}), which were highly abundant in Reloncaví Fjord. The small dinoflagellates, along with tintinnids, aloricate choeotrich ciliates (i.e. *Strombidium* sp.) and HNF constituted some of the main food items for copepods in winter, when PP levels dropped dramatically. On the contrary, chain-forming diatoms dominated the copepod diet during the productive season (spring), highlighting the adaptation of copepods, which are able to adjust their metabolic demands to the *in situ* availability of prey (Vargas et al. 2008). The strong halocline defines a natural barrier with an upper brackish layer dominated by small copepods and cladocerans and a lower layer dominated by marine copepods and euphausiids. The mesozooplankton grazing impact was mainly due to the euphausiid species *Euphausia vallentini*, which removed from ~2 (spring) to 38% (winter) of the PP daily at the process station (Table 3, Fig. 7). The grazing impact of calanoid copepods in this study was very low (≤1% PP), which lies in the lower range of values reported (<2 to 92% PP) (see Table 4), probably because few species of calanoid copepods *Acartia* and *Calanus* were studied. Small cyclopod copepods (i.e. *Oithona* spp.) were not included in this study, despite their numerical dominance in disparate estuarine systems (Maar et al. 2004), because the zooplankton nets we used were too coarse (300 and 200 µm mesh) to adequately collect such small copepods.

From winter to spring, the BSP:PP ratio decreased from 3.7 to 0.2 at the process station, but remained low (<0.1) year-round at the Desertores Islands (Stn 20). As the heterotrophic bacteria biomass did not change substantially, local topographic effects associated with these islands (i.e. retention eddies or sill/contraction topography) probably provoked the highest chl *a* values due to physical accumulation (Fig. 5A). The effects of sills and channels (sluggish flushing and particle accumulation) have been reported for the Chilean fjord region (Cáceres & Valle-Levinson 2004). Overall, seasonal changes in this ratio are related more to sharp spring-to-winter decreases in PP than to changes in bacterial biomass or production.

The average POC concentrations in the upper 50 m of the water column (spring–summer) decreased from 200–600 mgC m^{-3} around Reloncaví Fjord to 76 mgC m^{-3} (Fabiano et al. 1999) around the Strait of Magellan, appearing to parallel the percentage of organic carbon in the sediments from the same areas (from 5.3 to 3.8%, respectively, Silva & Prego 2002). These gradients could be due to more efficient pelagic-benthic coupling in the northern than in the southern Patagonian fjords given the (1) higher PP, (2) increased diatom abundances that resulted in high vertical POC fluxes, and (3) elevated light radiation, a precursor of allochthonous DOC flocculation and, in turn, carbon sequestration (von Wachenfeldt et al. 2008).

Fate of autotroph-generated PP and pelagic-benthic coupling in Reloncaví Fjord

In Reloncaví Fjord, the POC vertical flux was ca. 2-fold higher in spring than in winter (725 vs. 334 mgC m^{-2} d^{-1}, Table 3), whereas the PP was 40 times higher. This indicates that the POC export depended more on the variable input of both particulate and dissolved matter from terrestrial systems and was more uncoupled from local PP than in coastal areas. This was evi-

dent in the nearby Puyuhuapi Fjord, where surface sediments contain up to 50% terrestrial material (Sepúlveda et al. 2005). Microscopic analyses of sediment trap samples showed that faecal pellets from zooplankton (euphausiids, copepods, appendicularians) constituted the main vehicle for POC export towards the deeper layers of the Fjord, resembling the pivotal role of faecal material reported for coastal areas in the central-northern Humboldt Current System off Chile (González et al. 2004, 2007) and other fjords such as Conception Bay, Newfoundland, Canada, where the importance of zooplankton grazing to the phaeopigment flux was suggested by the predominance of phaeopigments in terms of total pigments (Thompson et al. 2008). On average, the export flux fluctuated from 500% (winter) to 33% (spring) of the PP. The high POC flux estimated in the Reloncaví Fjord lies in the upper range of the reported fluxes for other estuarine and fjord systems (Table 4) and may affect higher trophic layers, particularly benthic communities, and CO_2 sequestration in spring.

Carbon fluxes and fjord-system functioning are highly variable on a seasonal basis (Fig. 7), and the overall picture that emerged from our study showed high solar radiation in spring and an extended photoperiod that promoted the growth of chain-forming diatoms in a nutrient-repleted water column, in which silicic acid, DOM and POM were provided by freshwater input. Allochthonous (river discharge) and autochthonous (phytoplankton exudates) OM kept the bacterial biomass and secondary production high yearround. In spring, high PP and the grazing pressure of zooplankton (mainly *Euphausia vallentini*) on the diatom-dominated microplankton resulted in a relative dominance of the classical food web, with increased export production. Conversely, in winter, low PP, high HNF bacterivory rates and zooplankton grazing on nanoplankton (both auto- and heterotrophic) resulted in a relative dominance of the microbial loop with lower (than in spring) export production.

Acknowledgements. We thank the entire crew and all the scientists of the CIMAR 12-2006 oceanographic cruise. We thank María Inés Muñoz and Hector Paves for euphausiid and copepod analysis, respectively. We also thank Lorena Rebolledo for sharing with us unpublished data on stable isotope in sediment cores from the Reloncaví Fjord, and Jorge León, Nicolás Sánchez and Ricardo Giesecke for stimulating discussions on plankton dynamics in Patagonian systems. This study was funded by the project CIMAR12-Fiordos (CONA-SHOA, Chile). Additional support is also acknowledged from COPAS grant FONDAP-15010007 and COPAS Sur-Austral grant PFB-31/2007.

LITERATURE CITED

Acha EM, Mianzan HW, Guerrero RA, Favero M, Bava J (2004) Marine fronts at the continental shelves of austral South America: physical and ecological processes. J Mar Syst 44:83–105

Álvarez-Salgado XA, Nieto-Cid M, Piedracoba S, Crespo BG and others (2005) Origin and fate of a bloom of *Skeletonema costatum* during a winter upwelling/downwelling sequence in the Ría de Vigo (NW Spain). J Mar Res 63: 1127–1149

Antezana T (1999) Plankton of southern Chilean fjords: trends and linkages. Sci Mar 63:69–80

Archer SD, Verity PG, Stefels J (2000) Impact of microzooplankton on the progression and fate of the spring bloom in fjords of northern Norway. Aquat Microb Ecol 22:27–41

Atlas ES, Hager S, Gordon L, Park P (1971) A practical manual for use of the Technicon Autoanalyser in sea water nutrient analyses. Deptartment of Oceanography. Technical Report, Oregon State University, Corvallis, OR

Avaria S, Jorquera L, Muñoz P, Vera P (1999) Distribución del microfitoplancton marino en la zona de aguas interiores comprendidas entre el golfo de Penas y el Estrecho de Magallanes, Chile, en la primavera de 1996 (Crucero Cimar-Fiordo 2). Cien Tecnol Mar 22:81–109

Balbontín F, Bernal R (1997) Distribución y abundancia del ictioplancton en la zona austral de Chile. Cien Tecnol Mar 20:155–163

Basten J, Clement A (1999) Oceanografía del Estuario de Reloncaví, X Región de Chile. Cien Tecnol Mar 22:31–46

Børsheim KY, Bratbak G (1987) Cell volume to cell carbon conversion factor for a bacterivorous *Monas* sp. enriched from seawater. Mar Ecol Prog Ser 36:171–175

Cáceres A, Valle-Levinson A (2004) Transverse variability of flow on both sides of a sill/contraction combination in a fjord-like inlet of southern Chile. Estuar Coast Shelf Sci 60:325–338

Calbet A, Landry MR (2004) Phytoplankton growth, microzooplankton grazing, and carbon cycling in marine systems. Limnol Oceanogr 49:51–57

Ducklow HW, Smith DC, Campbell L, Landry MR, Quinby HL, Steward GF, Azam F (2001) Heterotrophic bacterioplankton in the Arabian Sea: basinwide response to yearround high primary productivity. Deep-Sea Res II 48: 1303–1323

Edler L (1979) Recommendations for marine biological studies in the Baltic Sea. Balt Mar Biol Publ 5:11–38

Eppley RW, Rogers JN, McCarthy JJ (1969) Half-saturation constants for uptake of nitrate and ammonium by marine phytoplankton. Limnol Oceanogr 12:685–695

Escribano R, Fernandez M, Aranís A (2003) Physical-chemical processes and patterns of diversity of the chilean eastern boundary pelagic and benthic marine ecosystems: an overview. Gayana (Zool) 67:190–205

Fabiano M, Povero P, Danovaro R, Misic C (1999) Particulate organic matter composition in a semi-enclosed Periantarctic system: the Straits of Magellan. Sci Mar 63:89–98

Frost BW (1972) Effects of size and concentration of food particles on the feeding behaviour of the marine planktonic copepod *Calanus pacificus.* Limnol Oceanogr 17:805–815

Gifford DJ (1993) Consumption of protozoa by copepod feeding on natural microplankton assemblages. In: Kemp PF, Sherr BF, Sherr EB, Cole JJ (eds) Handbook of methods in aquatic microbial ecology. Lewis Publishers, London, p 723–737

Gifford DJ, Caron DA (2000) Sampling, preservation, enumeration and biomass of marine protozooplankton. In: Harris RP, Wiebe PH, Lenz J, Skjoldal HR, Huntley M (eds) ICES zooplankton methodology manual. Academic Press, New York, p 193–221

González HE, Bernal P, Ahumada R (1987) Desarrollo de do-

minancia locales la taxocenosis fitoplanctónica de la Bahía de Concepción, Chile, durante un evento de surgencia costera. Rev Chil Hist Nat 60:19–35

González HE, Pantoja S, Iriarte JL, Bernal P (1989) Winter-spring variability of size-fractionated autotrophic biomass in Concepción Bay, Chile. J Plankton Res 11:1157–1167

González HE, González SR, Brummer GJ (1994) Short-term sedimentation pattern of zooplankton, faeces and microplankton at a permanent station in the Bjørnafjorden (Norway) during April–May 1992. Mar Ecol Prog Ser 105: 31–45

González HE, Sobarzo M, Figueroa D, Nöthig EM (2000) Composition, biomass and potential grazing impact of the crustacean and pelagic tunicates in the northern Humboldt Current area off Chile: differences between El Niño and non-El Niño years. Mar Ecol Prog Ser 195:201–220

González HE, Hebbeln D, Iriarte JL, Marchant M (2004) Downward fluxes of faecal material and microplankton at 2300 m depth in the oceanic area off Coquimbo (30° S), Chile, during 1993–1995. Deep-Sea Res II 51:2457–2474

González HE, Menschel E, Aparicio C, Barría C (2007) Spatial and temporal variability of microplankton and detritus, and their export to the shelf sediments in the upwelling area off Concepción, Chile (~36° S), during 2002–2005. Prog Oceanogr 75:435–451

González HE, Daneri G, Iriarte JL, Yannicelli B and others (in press) (2009) Carbon fluxes within the epipelagic zone of the Humboldt Current System off Chile: the significance of euphausiids and diatoms as key functional groups for the biological pump. Prog Oceanogr 83:217–227

Haas LW (1982) Improved epifluorescence microscopy for observing planktonic microorganisms. Ann Inst Oceanogr 58:261–266

Hamamé M, Antezana T (1999) Chlorophyll and zooplankton in micro basins along the Strait of the Magellan–Beagle Channel passage. Sci Mar 63:35–42

Hirst AG, Roff JC, Lampitt RS (2003) A synthesis of growth rates in marine epipelagic invertebrate zooplankton. Adv Mar Biol 44:1–142

Hoffman JC, Bronk DA, Olney JE (2008) Organic matter sources supporting lower food web production in the tidal freshwater portion of the York River Estuary, Virginia. Estuar Coasts 31:898–911

Iriarte JL, Kusch A, Osses J, Ruiz M (2001) Dynamics of phytoplankton in the subantarctic area of the Straits of Magellan (53°S), Chile, during spring-summer 1997–98. Polar Biol 24:154–162

Iriarte JL, González HE, Liu KK, Rivas C, Valenzuela C (2007) Spatial and temporal variability of chlorophyll and primary productivity in surface waters of southern Chile (41.5–43°S). Estuar Coast Shelf Sci 74:471–480

Kivi K, Setala O (1995) Simultaneous measurement of food particle selection and clearance rates of planktonic oligotrich ciliates (Ciliophora: Oligotrichina). Mar Ecol Prog Ser 119:125–137

Lara A, Villalba R, Urrutia R (2008) A 400-year tree-ring record of the Puelo River summer–fall streamflow in the Valdivian Rainforest eco-region, Chile. Clim Change 86: 331–356

Lee S, Fuhrman J (1987) Relationship between biovolume and biomass of naturally-derived marine bacterioplankton. Appl Environ Microbiol 53:1298–1303

Maar M, Nielsen TG, Gooding S, Tönnesson K and others (2004) Trophodynamic function of copepods, appendicularians and protozooplankton in the late summer zooplankton community in the Skagerrak. Mar Biol 144: 917–933

Maranger RJ, Pace ML, del Giorgio PA, Caraco NF, Cole JJ (2005) Longitudinal spatial patterns of bacterial production and respiration in a large river-estuary: implications for ecosystem carbon consumption. Ecosystems 8:318–330

Marín V, Antezana T (1985) Species composition and relative abundance of copepods in Chilean fjords. J Plankton Res 7:961–966

Marín V, Huntley ME, Frost B (1986) Measuring feeding rates of pelagic herbivores: analysis of experimental design and methods. Mar Biol 93:49–58

Mujica A, Medina M (2000) Distribución y abundancia de larvas de crustáceos decápodos en el zooplancton de los canales australes. Proyecto Cimar-Fiordo 2. Cien Tecnol Mar 23:49–68.

Nielsen TG, Andersen CM (2002) Plankton community structure and production along a freshwater-influenced Norwegian fjord system. Mar Biol 141:707–724

Nielsen TG, Richardson K (1989) Food chain structure of the North Sea plankton communities: seasonal variations of the roles of the microbial loop. Mar Ecol Prog Ser 56:75–88

Ohman MD, Snyder RA (1991) Growth kinetics of the omnivorous oligotrich ciliate *Strombidium* sp. Limnol Oceanogr 36:922–935

Paasche E (1973) Silicon and ecology of marine plankton diatoms. II. Silicate-uptake kinetics in five diatom species. Mar Biol 19:262–269

Painting SJ, Moloney CL, Probyn TA, Tibbles B (1992) Microheterotrophic pathways in the southern Benguela upwelling system. In: Payne AIL, Brink KH, Mann KH, Hilborn R (eds) Benguela trophic functioning. S Afr J Mar Sci 12:527–543

Palma S, Aravena G (2001) Distribución de sifonóforos, quetognatos y eufáusidos en la región magallánica. Cien Tecnol Mar 24:47–59

Palma S, Silva N (2004) Distribution of siphonophores, chaetognaths, euphausiids and oceanographic conditions in the fjords and channels of southern Chile. Deep-Sea Res II 51:513–535

Pantoja S, Iriarte JL, Gutiérrez M, Calvete C (2010) The Southern Chile continental margin. In: Liu KK, Atkinson L, Quiñones R, Talaue-McManus L (eds) Carbon and nutrient fluxes in continental margins: a global synthesis. Global change. The IGBP Series, Springer Verlag, Berlin, p 265–272

Parsons TR, Maita R, Lalli CM (1984) Counting, media and preservation. A manual of chemical and biological methods for seawater analysis. Pergamon Press, Toronto

Paves HJ, González HE (2008) Carbon fluxes within the pelagic food web in the coastal area off Antofagasta (23°S), Chile: the significance of the microbial versus classical food webs. Ecol Model 212:218–232

Perakis SS, Hedin LO (2002) Nitrogen loss from unpolluted South American forests via dissolved organic compounds. Nature 415:416–419

Pickard GL (1971) Some physical oceanographic features of inlets of Chile. J Fish Res Board Can 28:1077–1106

Pizarro G, Iriarte JL, Montecino V, Blanco JL, Guzmán L (2000) Distribución de la biomasa fitoplanctónica y productividad primaria máxima de fiordos y canales australes (47°–50°S) en octubre 1996. Cien Tecnol Mar 23:25–47

Porter KG, Feig YS (1980) The use of DAPI for identifying and counting aquatic microflora. Limnol Oceanogr 25:943–948

Raymond PA, Bauer JE (2000) Bacterial consumption of DOC during transport through a temperate estuary. Aquat Microb Ecol 22:1–12

Rosenberg P, Palma S (2003) Cladóceros de los fiordos y canales patagónicos localizados entre el golfo de Penas y

el Estrecho de Magallanes. Invest Mar Valparaíso 31: 15–24

Ryther JH (1969) Photosynthesis and fish production in the sea. Science 166:72–76

Sánchez N (2007) Variación estacional y tasas de ingestión del zooplancton quitinoso dominante en el fiordo Comau (X Región, Chile), durante 2005–2007. Marine Biology thesis, Universidad Austral de Chile, Valdivia

Sato M, Yoshikawa T, Takeda S, Furuya K (2007) Application of the size-fractionation method to simultaneous estimation of clearance rates by heterotrophic flagellates and ciliates of pico- and nanophytoplankton. J Exp Mar Biol Ecol 349:334–343

Sepúlveda J, Pantoja S, Hughen K, Lange C and others (2005) Fluctuations in export productivity over the last century from sediments of a southern Chilean fjord (44°S). Estuar Coast Shelf Sci 65:587–600

Shikata T, Nagasoe S, Matsubara T, Yoshikawa S and others (2008) Factors influencing the initiation of blooms of the raphidophyte *Heterosigma akashivo* and the diatom *Skeletonema costatum* in a port in Japan. Limnol Oceanogr 53:2503–2518

Silva N, Neshyba S (1979) On the southernmost extension of the Perú-Chile Undercurrent. Deep-Sea Res 26:1387–1393

Silva N, Palma S (2006) Avances en el conocimiento oceanográfico de las aguas interiores chilenas, Puerto Montt a Cabo de Hornos. Comité Oceanográfico Nacional–Pontificia Universidad Católica de Valparaíso, Valparaíso, p 162

Silva N, Prego R (2002) Carbon and nitrogen spatial segregation and stoichiometry in the surface sediments of southern Chilean inlets (41°–56°S). Estuar Coast Shelf Sci 55: 763–775

Silva N, Calvete C, Sievers H (1997) Características oceanográficas físicas y químicas de canales australes chilenos entre Puerto Montt y Laguna San Rafael (Crucero Cimar Fiordo 1). Cien Tecnol Mar 20:23–106

Silva N, Calvete C, Sievers HA (1998) Masas de agua y circulación general para algunos canales australes entre Puerto Montt y Laguna San Rafael, Chile (Crucero Cimar-Fiordo 1). Cien Tecnol Mar 21:17–48

Silva N, Haro J, Prego R (2009) Metals background and enrichment in the Chiloé Interior Sea sediments (Chile). Is there any segregation between fjords, channels and sounds? Estuar Coast Shelf Sci 82:469–476

Simon M, Azam F (1989) Protein content and protein synthesis rates of planktonic marine bacteria. Mar Ecol Prog Ser 51:201–213

Smetacek V, von Bröckel K, Zeitzschel B, Zenk W (1978) Sedimentation of particulate matter during a phytoplankton spring bloom in relation to the hydrographical regime. Mar Biol 47:211–226

Tarutani K, Yamamoto T (1994) Phosphate uptake and growth kinetics of *Skeletonema costatum* isolated from Hiroshima Bay. J Fac Appl Biol Sci Hiroshima Univ 33:59–64

Thompson RJ, Deibel D, Redden AM, McKenzie CH (2008) Vertical flux and fate of particulate matter in a Newfoundland fjord at sub-zero water termperatures during spring. Mar Ecol Prog Ser 357:33–49

Tian RC, Vezina AF, Starr M, Saucier F (2001) Seasonal dynamics of coastal ecosystems and export production at high latitudes: a modeling study. Limnol Oceanogr 46: 1845–1859

Troncoso VA, Daneri G, Cuevas LA, Jacob B, Montero P (2003) Bacterial carbon flow in the Humboldt Current System off Chile. Mar Ecol Prog Ser 250:1–12

Turner JT (2002) Zooplankton faecal pellets, marine snow and sinking phytoplankton blooms. Aquat Microb Ecol 27: 57–102

Utermöhl H (1958) Zur Vervollkommnung der quantitativen Phytoplankton–Methodik. Mitt Int Ver Theor Angew Limnol 9:1–39

Uye SI, Nagano N, Hidenori TH (1996) Geographical and seasonal variations in abundance, biomass and estimated production rates of microzooplankton in the Inland Sea of Japan. J Oceanogr 52:689–703

Vargas CA, González HE (2004) Plankton community structure and carbon cycling in a coastal upwelling system. II. Microheterotrophic pathway. Aquat Microb Ecol 34: 165–180

Vargas CA, Martínez R, Cuevas LA, Pavez M and others (2007) The relative importance of microbial and classical food webs in a highly productive coastal upwelling area. Limnol Oceanogr 52:1495–1510

Vargas CA, Martínez R, González HE, Silva N (2008) Contrasting trophic interactions of microbial and copepod communities in a fjord ecosystem (Chilean Patagonia). Aquat Microb Ecol 53:227–242

Verity P, Langdon C (1984) Relationship between lorica volume, carbon, nitrogen, and ATP content of tintinnids in Narragansett Bay. J Plankton Res 6:859–868

von Bodungen B, Wunsch M, Fürderer H (1991) Sampling and analysis of suspended and sinking particles in the northern North Atlantic. In: Hurd DC, Spencer DW (eds) Marine particles: analysis and characterization. AGU Geophys Monogr 63:47–56

von Wachenfeldt E, Sobeck S, Bastviken D, Tranvik LJ (2008) Linking allochthonous dissolved organic matter and boreal lake sedimentation carbon sequestration: the role of light mediated flocculation. Limnol Oceanogr 53: 2416–2426

Editorial responsibility: Peter Verity, Savannah, Georgia, USA

Submitted: May 14, 2009; Accepted: October 6, 2009
Proofs received from author(s): February 19, 2010